WCCM XI - ECCM V - ECFD VI
BARCELONA 2014

11th. World Congress on Computational Mechanics

Convergence analysis of configurational forces for brittle cracks modeled through C^k-Generalized FEM

Diego Amadeu F. Torres

Clovis S. de Barcellos

Paulo de Tarso R. Mendonça

UFSC

Department of Mechanical Engineering

Federal University of Santa Catarina

Brazil

Presentation topics

- Construction of continuous **Partition of Unity** at C^k-GFEM
- Construction of a smooth approximation subspace
- Elshebian mechanics as tool to post-processing of J-integral
- Quality assessment through **global** and **local measures**
- Concluding remarks

GFEM/XFEM versus C^k-GFEM

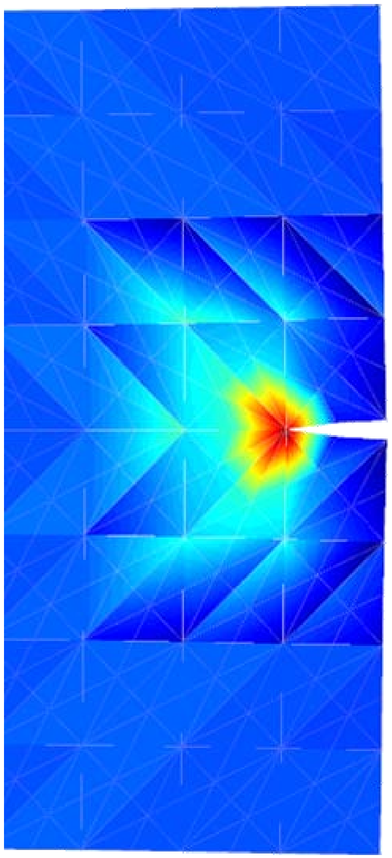

- Regularity;
- Polynomial reproducibility;
- Efficient enrichment patterns;
- Flat-top property;
- Integration cost;
- Integration of C^0 and C^k-GFEM.

WCCM XI - ECCM V - ECFD VI
BARCELONA 2014

C^k partition of unity – convex clouds

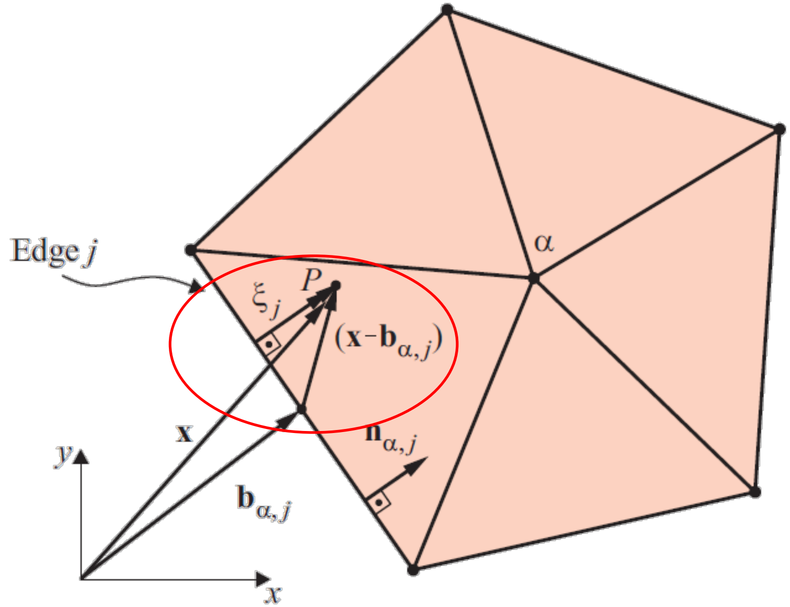

Arbitrary patch shape;
Arbitrary element shape;
free of coordinate mapping;

$$\xi_j(\boldsymbol{x}) = \boldsymbol{n}_{\alpha,j} \cdot (\boldsymbol{x} - \boldsymbol{b}_{\alpha,j})$$

$$\varepsilon_{\alpha,j}[\xi_j(\mathbf{x})] = \widehat{\varepsilon}_{\alpha,j}(\mathbf{x}) := \begin{cases} e^{-\xi_j^{-\gamma}} & \text{if } 0 < \xi_j \\ 0, & \text{otherwise} \end{cases}$$ $k = \infty$

$$\varepsilon_{\alpha,j}[\xi_j(\mathbf{x})] = \widehat{\varepsilon}_{\alpha,j}(\mathbf{x}) := \begin{cases} (\xi_j/h_j)^{\mathrm{P}} & \text{if } 0 < \xi_j \\ 0, & \text{otherwise} \end{cases}$$ $k = p - 1$

Edwards, ***C*$^\infty$ *finite element basis functions***, Report 45,
Institute for Computational Engineering and Sciences – The University of Texas at Austin, 1996

Duarte, Kim and Quaresma, ***Arbitrarily smooth generalized finite element approximations***. Computer Methods in Applied Mechanics and Engineering, 196 (2006)

Barcellos, Mendonça and Duarte, ***A Ck continuous generalized finite element formulation applied to laminated Kirchhoff plate model***. Computational Mechanics, 44 (2009)

C^{∞} partition of unity – convex clouds

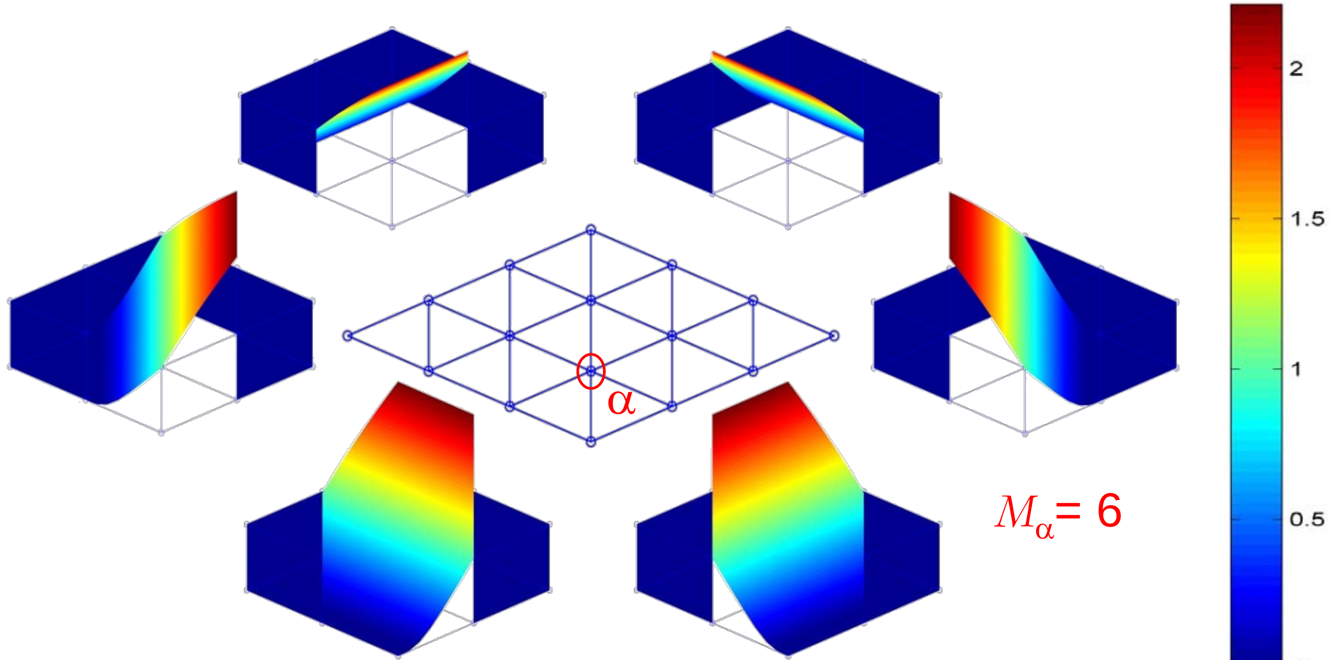

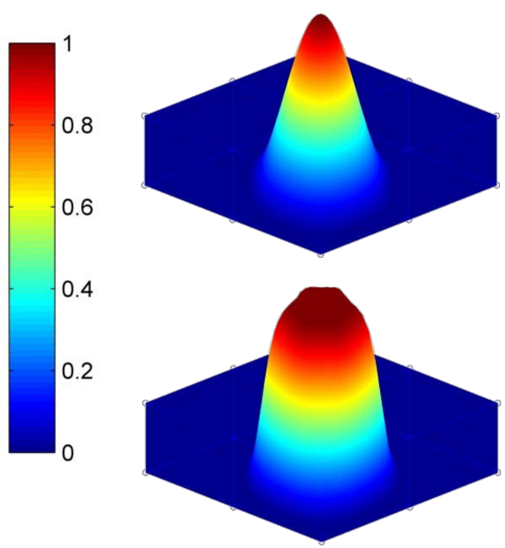

$$\mathcal{W}_\alpha(\boldsymbol{x}) := \prod_{j=1}^{M_\alpha} \varepsilon_{\alpha,j}\left(\xi_j\right)$$

$$\varphi_\alpha\left(\boldsymbol{x}\right) = \frac{\mathcal{W}_\alpha\left(\boldsymbol{x}\right)}{\sum_{\beta(\boldsymbol{x})} \mathcal{W}_\beta\left(\boldsymbol{x}\right)},$$

$$\beta\left(\boldsymbol{x}\right) \in \left\{\gamma \mid \mathcal{W}_\gamma\left(\boldsymbol{x}\right) \neq 0\right\}$$

Galerkin aproximation

$$\boldsymbol{u}_p(\boldsymbol{x}) = \sum_{\alpha=1}^{N} \varphi_\alpha(\boldsymbol{x}) \left\{ u_\alpha + \sum_{i=1}^{q_\alpha} \mathcal{L}_{\alpha i}(\boldsymbol{x}) b_{\alpha i} + \sum_{j=1}^{q_\alpha^s} \mathcal{L}_{\alpha j}^s b_{\alpha j}^s \right\}$$

if p=3 $\mathcal{L}_{\alpha 9}(x, y) = \left\{ \overline{x}, \overline{y}, \overline{x}^2, \overline{x}\,\overline{y}, \overline{y}^2, \overline{x}^3, \overline{x}^2\,\overline{y}, \overline{x}\,\overline{y}^2, \overline{y}^3 \right\}$

e.g. $\overline{x} := \dfrac{(x - x_\alpha)}{h_\alpha}$ for reducing mesh dependences

$q_\alpha^s = 4 \text{ or } 0$

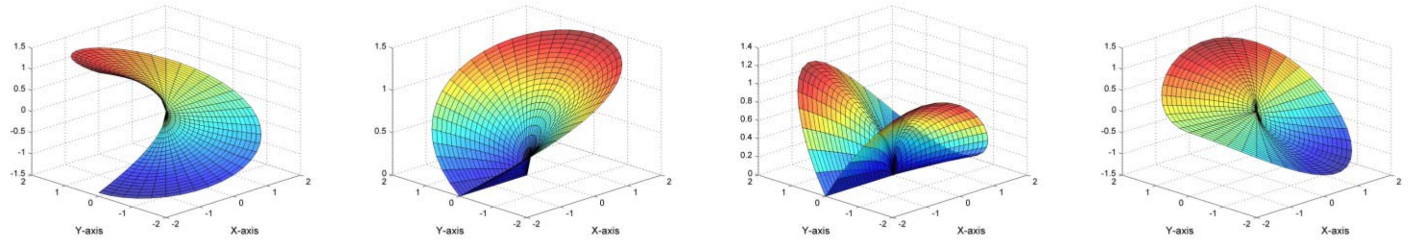

$$\mathcal{L}_{\alpha 4}^s(r, \theta) = \left\{ \sqrt{r}\sin\left(\frac{\theta}{2}\right), \sqrt{r}\cos\left(\frac{\theta}{2}\right), \sqrt{r}\sin\left(\frac{\theta}{2}\right)\sin(\theta), \sqrt{r}\cos\left(\frac{\theta}{2}\right)\sin(\theta) \right\}$$

Belytschko and Black, ***Elastic crack growth in finite elements with minimal remeshing***. International Journal for Numerical Methods in Engineering, 45 (1999)

Polynomial reproducibility of the approximation

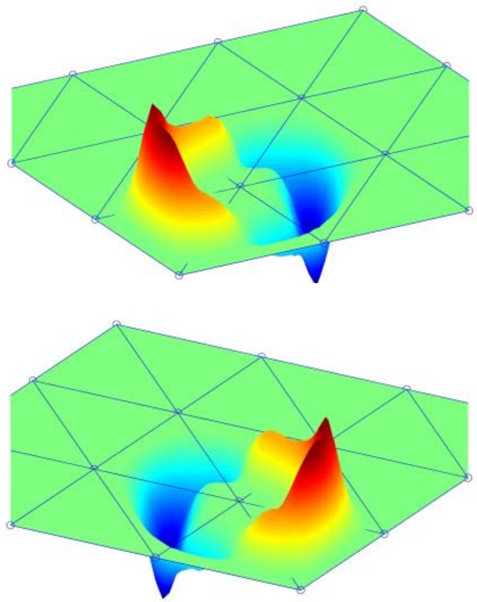

b=*p*+1 for C^0 PoU (conventional tent FEM shape function)

b=*p* for C^k PoU

p = degree of polynomial enrichment

Mendonça, Barcellos and Torres, ***Robust Ck/C0 generalized FEM approximations for higher-order conformity requirements: application to Reddy's HSDT model for anisotropic laminated plates***. Composite Structures, 96 (2013)

Mendonça, Barcellos and Torres, ***Analysis of anisotropic Mindlin plate model by continuous and non-continuous GFEM***. Finite Element in Analysis and Design, 47 (2011)

Barcellos, Mendonça and Duarte, ***A Ck continuous generalized finite element formulation applied to laminated Kirchhoff plate model***. Computational Mechanics, 44 (2009)

Geometric enrichment pattern

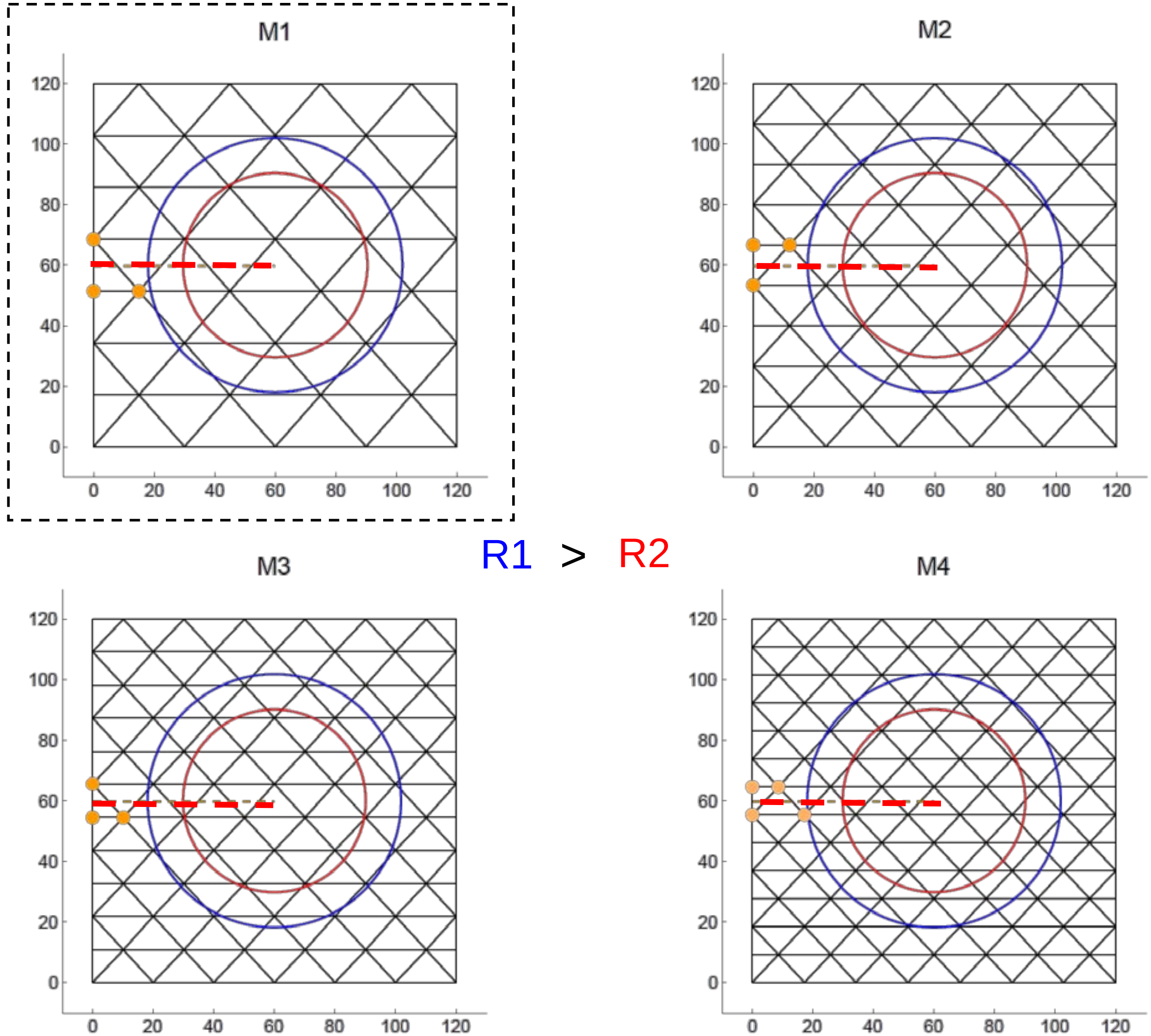

branch functions on orange nodes and inside the circles, and uniform polynomial enrichment

Continuous partition of unity with C^k-GFEM

Defining an approximation subspace

Quality assessment through global measures

Configurational forces method

Quality assessment through local measures

Smoothness, enrichments

Concluding remarks

Convergence in terms of global values

mode I opening crack loading

geometric pattern of singular enrichment

+

uniform polynomial enrichment

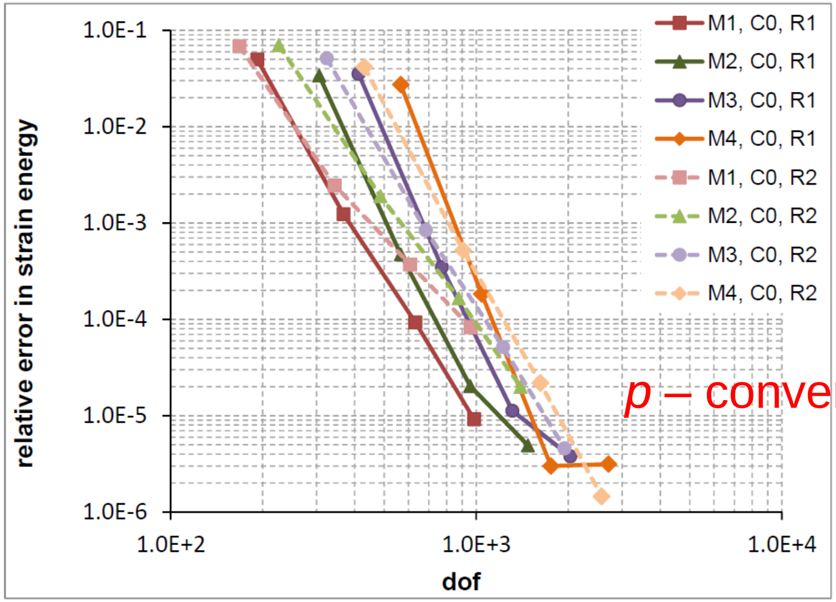

C^0

p – convergence !

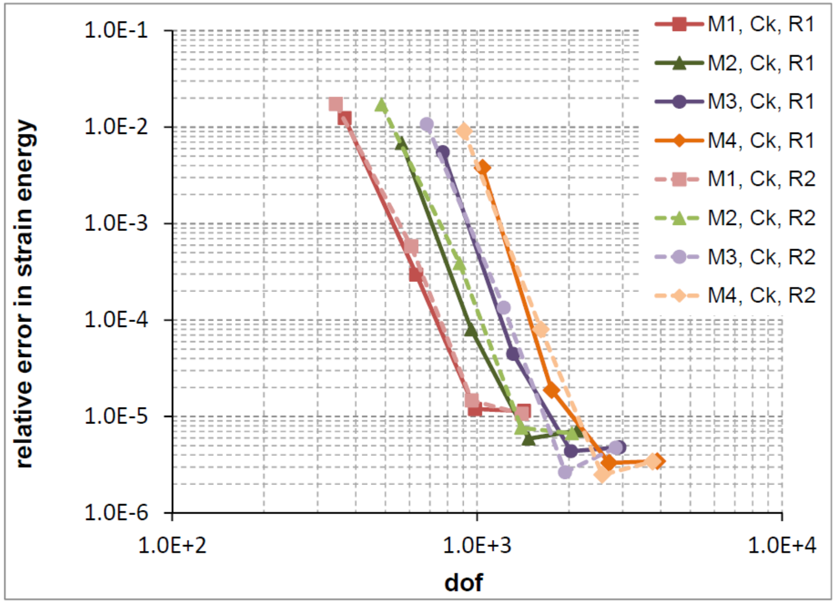

C^k

WCCM XI - ECCM V - ECFD VI
BARCELONA 2014

Configurational mechanics

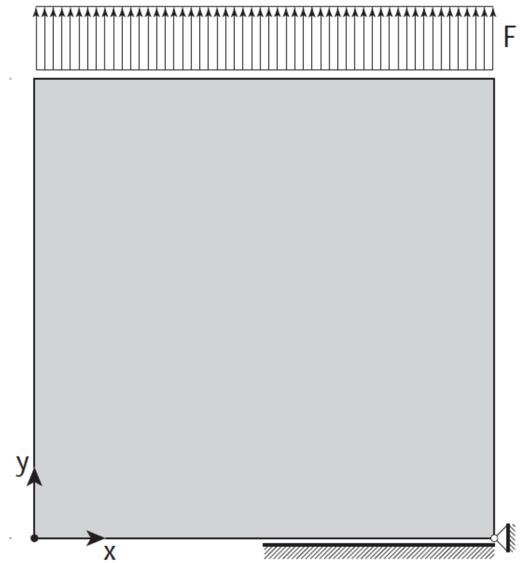

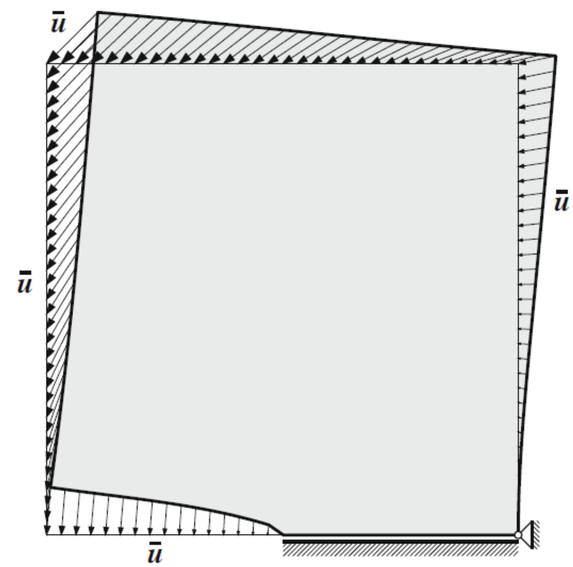

$$\boldsymbol{L}^T \boldsymbol{\sigma}(\boldsymbol{u}) + \boldsymbol{b} = \boldsymbol{0} \quad \text{, on } \Omega \qquad \mathbb{L}^T \boldsymbol{\Sigma}(\boldsymbol{u}) + \boldsymbol{\rho} = \boldsymbol{0} \quad \text{, on } \Omega$$

$$\boldsymbol{\sigma} = \{\sigma_x, \sigma_y, \tau_{xy}\}^T \;\; \boldsymbol{b} = \{b_x, b_y\}^T \qquad \boldsymbol{\Sigma} = \{\Sigma_x, \Sigma_y, \Sigma_{xy}, \Sigma_{yx}\}^T \;\; \boldsymbol{\rho} = \{\rho_x, \rho_y\}^T$$

Eshelby, ***The force on an elastic singularity.*** Philosophical Transactions of the Royal Society A: mathematical, physical and engineering sciences, 244 (1951)

Kienzler and Herrmann, ***Mechanics in material space with applications to defect and fracture mechanics.*** Springer, 2000

Ruter and Stein, ***On the duality of global finite element discretization error control in small strain Newtonial and Eshelbian mechanics.*** Technische Mechanik, 23 (2003)

WCCM XI - ECCM V - ECFD VI
BARCELONA 2014

Variational balance of material linear momentum

strong-form

$$\mathbb{L}^T \boldsymbol{\Sigma}(\boldsymbol{u}) + \boldsymbol{\rho} = \mathbf{0}$$

, where

$$\boldsymbol{\Sigma} = \{\Sigma_x, \Sigma_y, \Sigma_{xy}, \Sigma_{yx}\}^T$$

Eshelby tensor

$$\boldsymbol{\rho} = \{\rho_x, \rho_y\}^T$$

inhomogeneity force

$$\mathbb{L} = \begin{bmatrix} \frac{\partial}{\partial x} & 0 \\ 0 & \frac{\partial}{\partial y} \\ \frac{\partial}{\partial y} & 0 \\ 0 & \frac{\partial}{\partial x} \end{bmatrix}$$

and defining

$$\boldsymbol{\Sigma}(\boldsymbol{u}) = \mathfrak{W}(\boldsymbol{u})\, \underline{\mathbb{I}} - \underline{\mathbb{L}}^T(\boldsymbol{u})\, \boldsymbol{\sigma}(\boldsymbol{u})$$

$$\mathfrak{W} = \frac{1}{2}\boldsymbol{\sigma}^T \boldsymbol{\varepsilon} \qquad \underline{\mathbb{I}}^T = \{1, 1, 0, 0\}$$

$$\underline{\mathbb{L}}(\boldsymbol{u}) = \underline{\mathbf{L}}\, \underline{\mathbf{I}}\, \boldsymbol{u} \qquad \underline{\mathbf{L}} = \begin{bmatrix} \frac{\partial}{\partial x} & 0 & \frac{\partial}{\partial y} & 0 \\ 0 & \frac{\partial}{\partial y} & 0 & \frac{\partial}{\partial x} \\ \frac{\partial}{\partial x} & \frac{\partial}{\partial y} & \frac{\partial}{\partial y} & \frac{\partial}{\partial x} \end{bmatrix} \qquad \underline{\mathbf{I}} = \begin{bmatrix} 1 & 0 \\ 0 & 1 \\ 1 & 0 \\ 0 & 1 \end{bmatrix}$$

weak-form

$$\int_\Omega (\mathbb{L}\boldsymbol{v})^T \boldsymbol{\Sigma}\, l_z\, d\Omega = \int_\Omega (\boldsymbol{v})^T \boldsymbol{\rho}\, l_z\, d\Omega \qquad \boldsymbol{v} = \{v_x, v_y\}^T$$

Post-processing of nodal configurational forces

$$\int_{\Omega} (\mathbb{L}\boldsymbol{v})^T \boldsymbol{\Sigma}\, l_z \, d\Omega = \int_{\Omega} (\boldsymbol{v})^T \boldsymbol{\rho}\, l_z \, d\Omega \,, \quad \forall \boldsymbol{v} \mid \boldsymbol{v} = 0 \text{ on } \partial\Omega$$

Eshelby tensor $\boldsymbol{\Sigma}(\boldsymbol{u}) = \mathfrak{W}(\boldsymbol{u})\, \underline{\mathbb{I}} - \underline{\mathbb{L}}^T(\boldsymbol{u})\, \boldsymbol{\sigma}(\boldsymbol{u})$

$$\therefore \quad \sum_{\alpha=1}^{N} \mathbb{U}_\alpha^T \left[-\int\int_{\Omega^e} \mathbb{B}_\alpha^T \boldsymbol{\Sigma}\, l_z \, dx\, dy + \int\int_{\Omega^e} \widehat{\boldsymbol{\varphi}}_\alpha^T \boldsymbol{\rho}_\alpha \, l_z \, dx\, dy \right] = 0$$

where $\mathbb{B}_\alpha = \mathbb{L}\, \widehat{\varphi}_\alpha$

thus, defining

$$\boldsymbol{G}_\alpha^e = \left\{ \begin{array}{c} G_{x_\alpha}^e \\ G_{y_\alpha}^e \end{array} \right\} = \int\int_{\Omega^e} \widehat{\boldsymbol{\varphi}}_\alpha^T \boldsymbol{\rho}_\alpha \, l_z \, dx\, dy = \int\int_{\Omega^e} \mathbb{B}_\alpha^T \boldsymbol{\Sigma}\, l_z \, dx\, dy$$

$$\boldsymbol{G}_\alpha = \bigcup_{e=1}^{N_{ad}} \boldsymbol{G}_\alpha^e$$

nodal configurational force

Local measure using configurational forces

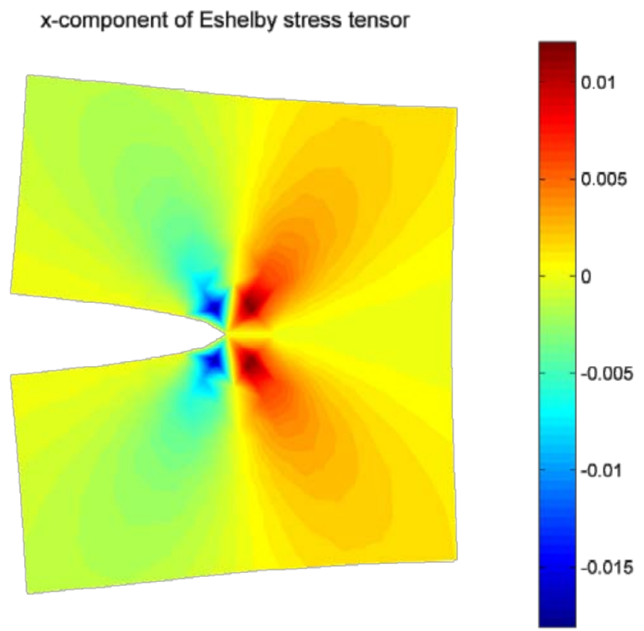

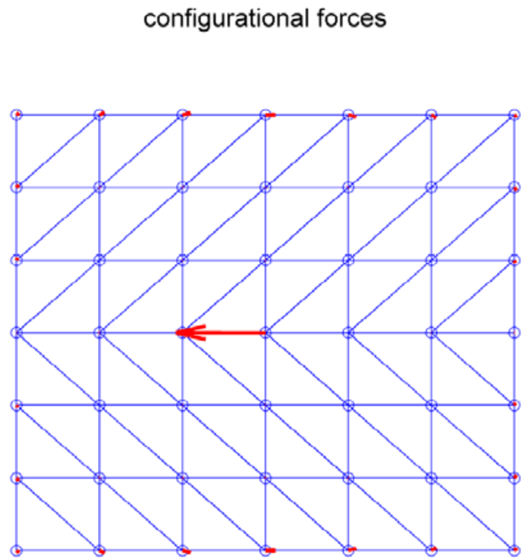

Eshelby, ***The force on an elastic singularity.*** Philosophical Transactions of the Royal Society A: mathematical, physical and engineering sciences, 244 (1951)

Kienzler and Herrmann, ***Mechanics in material space with applications to defect and fracture mechanics.*** Springer, 2000

Mueller and Maugin, ***On material forces and finite element discretizations.*** Computational Mechanics, 29 (2002)

Glaser and Steinmann, ***On material forces within the extended finite element method.*** Proceedings of the sixth European Solid Mechanics Conference (2006)

Häusler, Lindhorst and Horst, ***Combination of the material force concept and the extended finite element method for mixed mode crack growth simulations.*** International Journal for Numerical Methods in Engineering, 85 (2011)

Topologic enrichment pattern

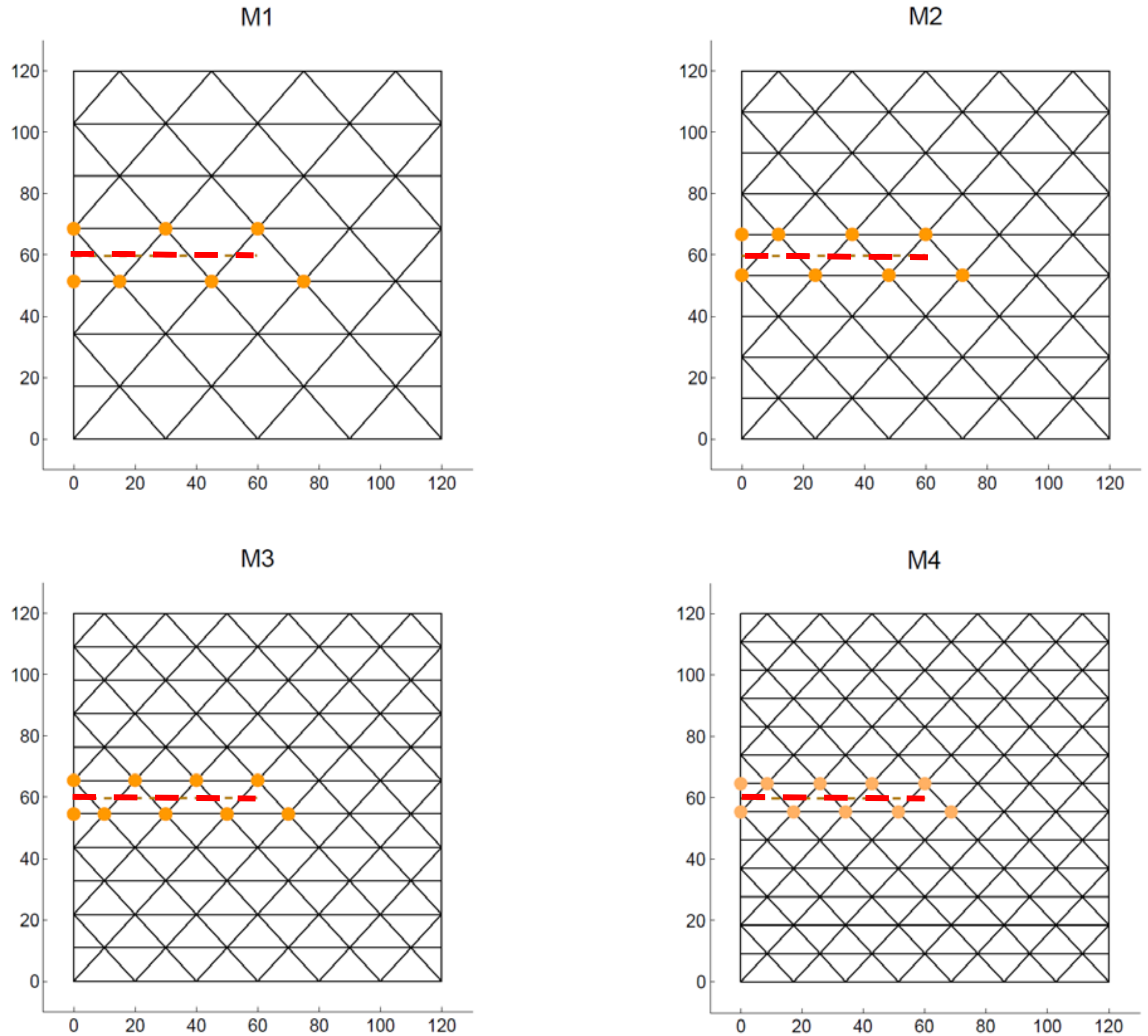

- Branch functions on orange nodes;
- Uniform *p*-enrichment
- Local *p*-enrichment around the crack tip

Mixed mode loading

$K_I = 1.0, \; K_{II} = 1.0$

$$\sigma_x = \frac{K_I}{\sqrt{2\pi r}} \cos\left(\frac{\theta}{2}\right)\left[1 - \operatorname{sen}\left(\frac{\theta}{2}\right)\operatorname{sen}\left(\frac{3\theta}{2}\right)\right] - \frac{K_{II}}{\sqrt{2\pi r}} \operatorname{sen}\left(\frac{\theta}{2}\right)\left[2 + \cos\left(\frac{\theta}{2}\right)\cos\left(\frac{3\theta}{2}\right)\right]$$

$$\sigma_y = \frac{K_I}{\sqrt{2\pi r}} \cos\left(\frac{\theta}{2}\right)\left[1 + \operatorname{sen}\left(\frac{\theta}{2}\right)\operatorname{sen}\left(\frac{3\theta}{2}\right)\right] + \frac{K_{II}}{\sqrt{2\pi r}} \operatorname{sen}\left(\frac{\theta}{2}\right)\cos\left(\frac{\theta}{2}\right)\cos\left(\frac{3\theta}{2}\right)$$

$$\tau_{xy} = \frac{K_I}{\sqrt{2\pi r}} \cos\left(\frac{\theta}{2}\right)\operatorname{sen}\left(\frac{\theta}{2}\right)\cos\left(\frac{3\theta}{2}\right) + \frac{K_{II}}{\sqrt{2\pi r}} \cos\left(\frac{\theta}{2}\right)\left[1 - \operatorname{sen}\left(\frac{\theta}{2}\right)\operatorname{sen}\left(\frac{3\theta}{2}\right)\right]$$

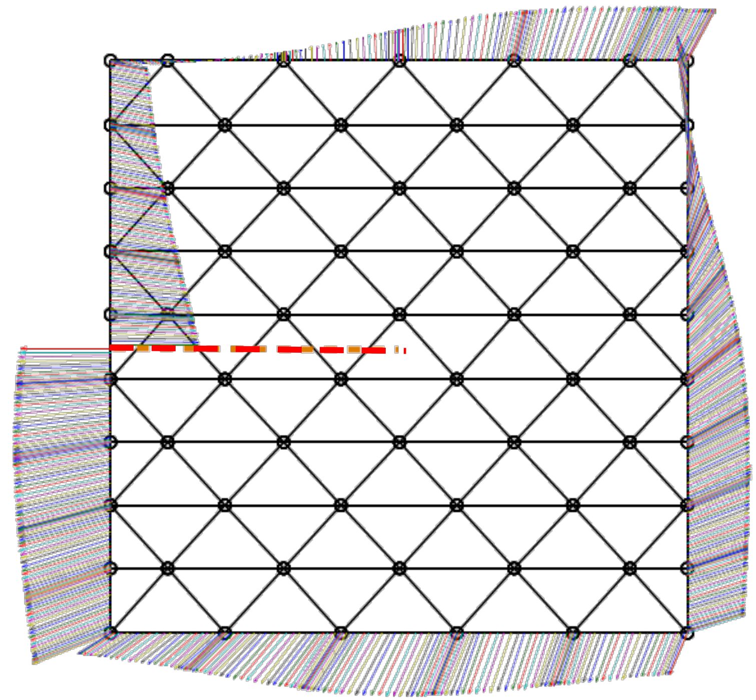

WCCM XI - ECCM V - ECFD VI
BARCELONA 2014

- Continuous partition of unity with C^k-GFEM
- Defining an approximation subspace
- **Quality assessment through global measures**
- Configurational forces method
- Quality assessment through local measures
- Smoothness, enrichments
- Concluding remarks

Convergence in global values

Topologic pattern of singular enrichment

+

Localized polynomial enrichment, *p*

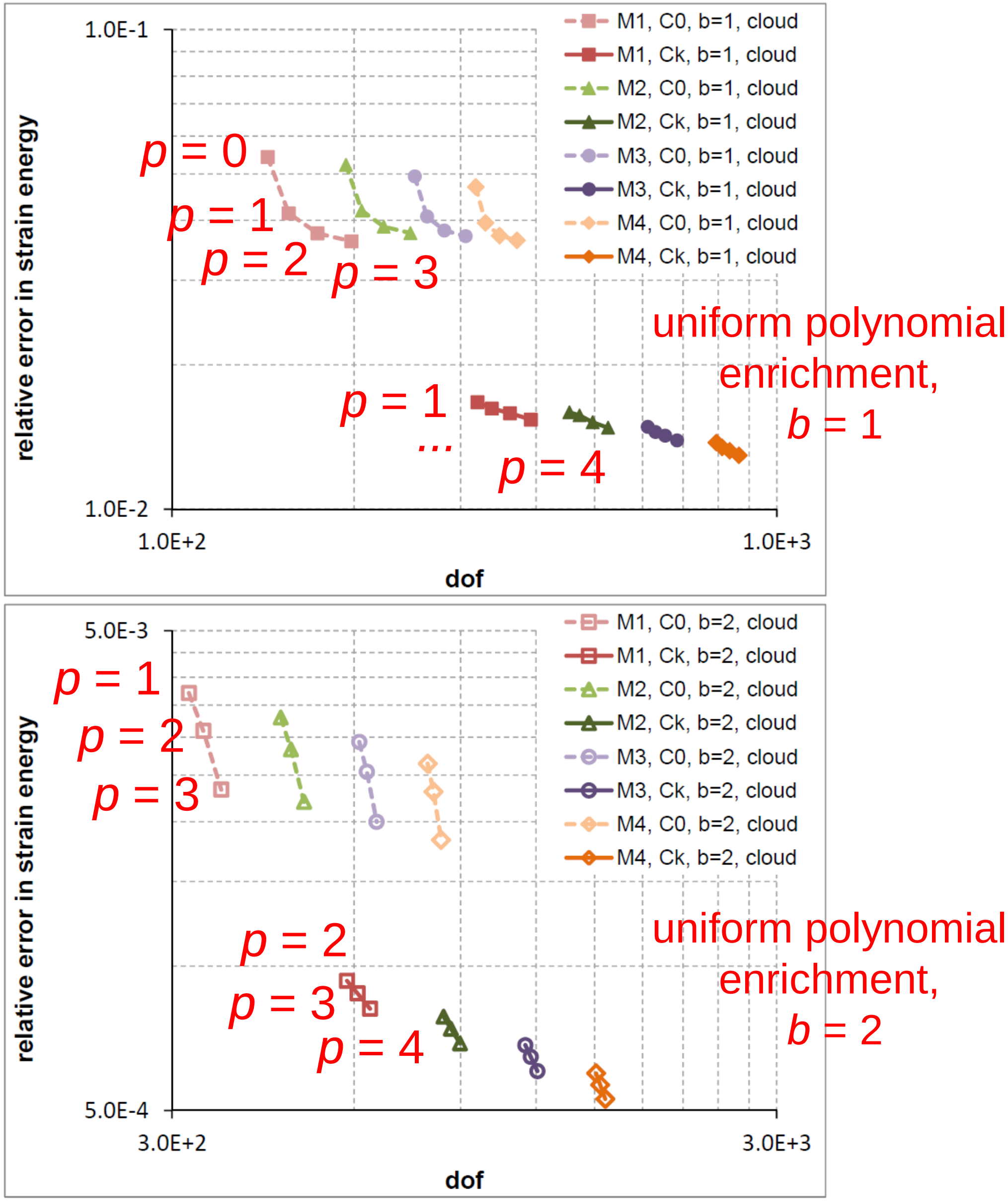

Convergence of J-integral

Topologic pattern of singular enrichment

+

Localized polynomial enrichment

$$\mathcal{R} = \left(K_I^2 + K_{II}^2\right) / E^*$$

$$E^* = E(1 - \nu^2)$$

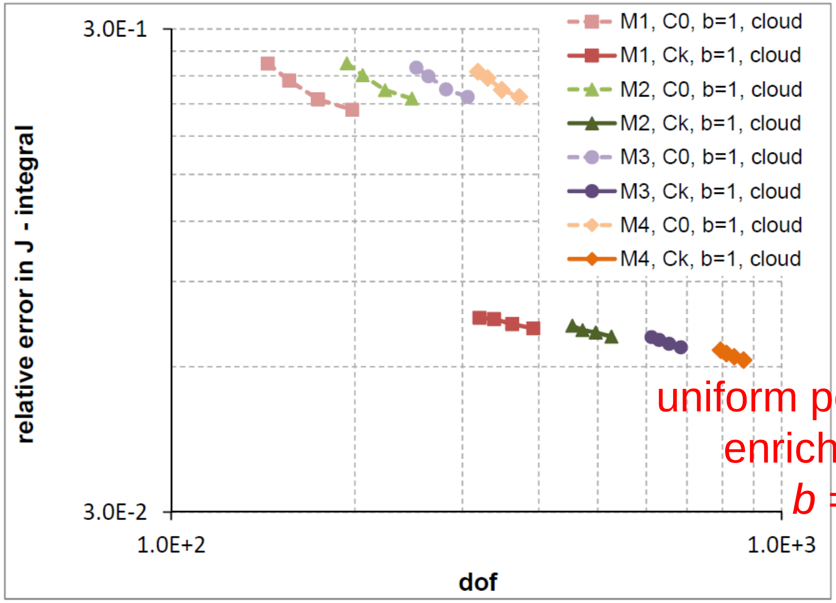

uniform polynomial enrichment, b = 1

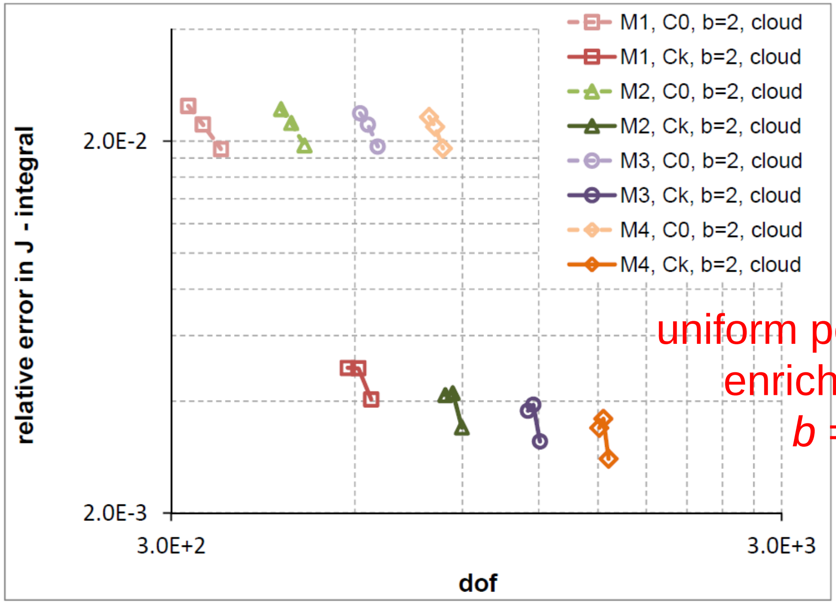

uniform polynomial enrichment, b = 2

Exact error dispersion: *y*-stress

Topologic pattern of singular enrichment

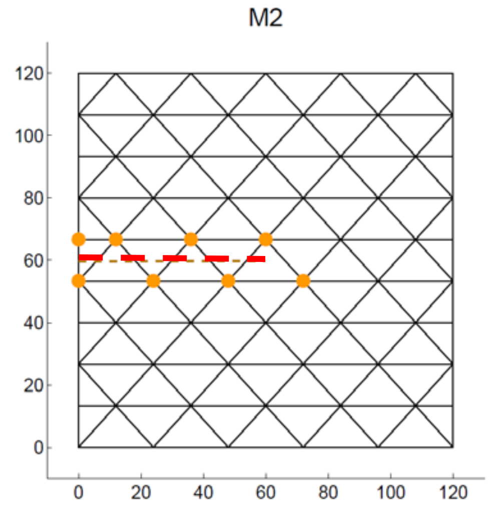

Uniform polynomial enrichment,
b = 1

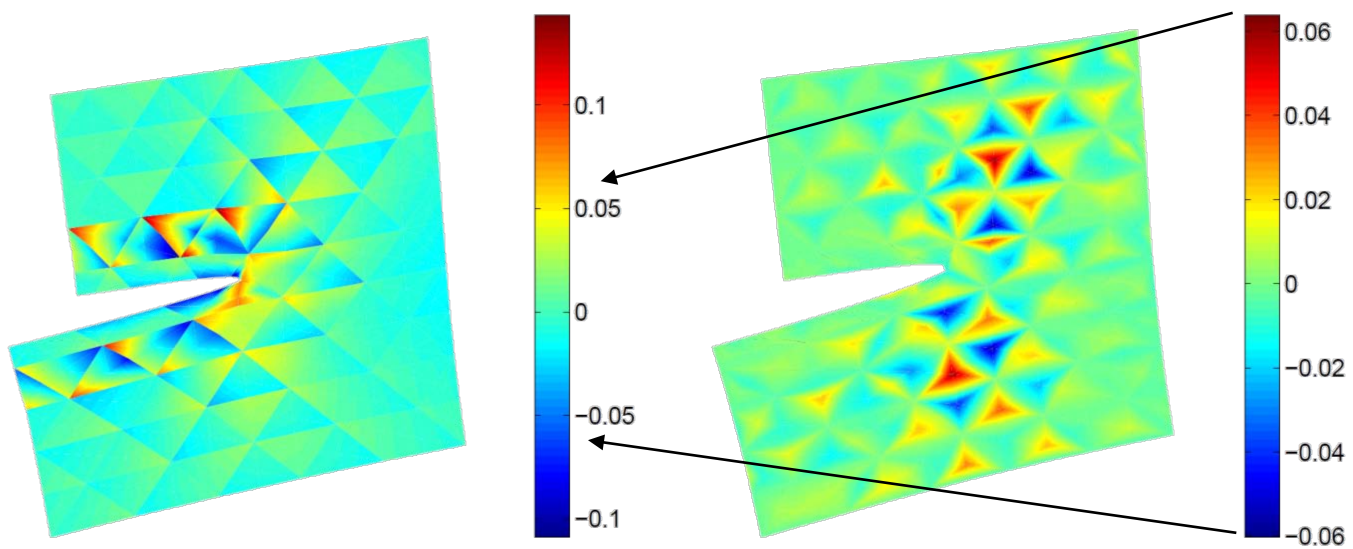

C0, 191 DOFs

C∞, 451 DOFs

Exact error dispersion: *y*-stress

topologic pattern of singular enrichment

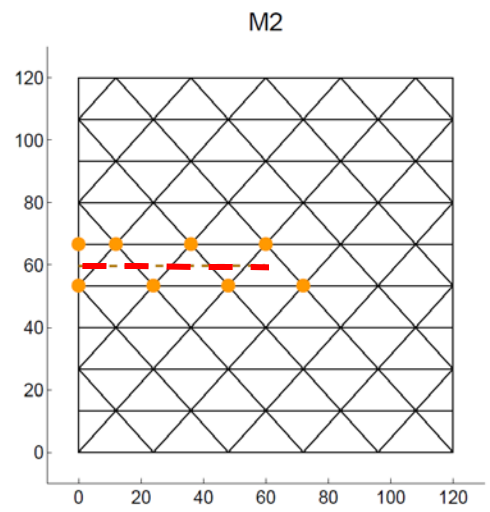

uniform polynomial enrichment, $b = 1$

+

localized polynomial enrichment, $p = 2$

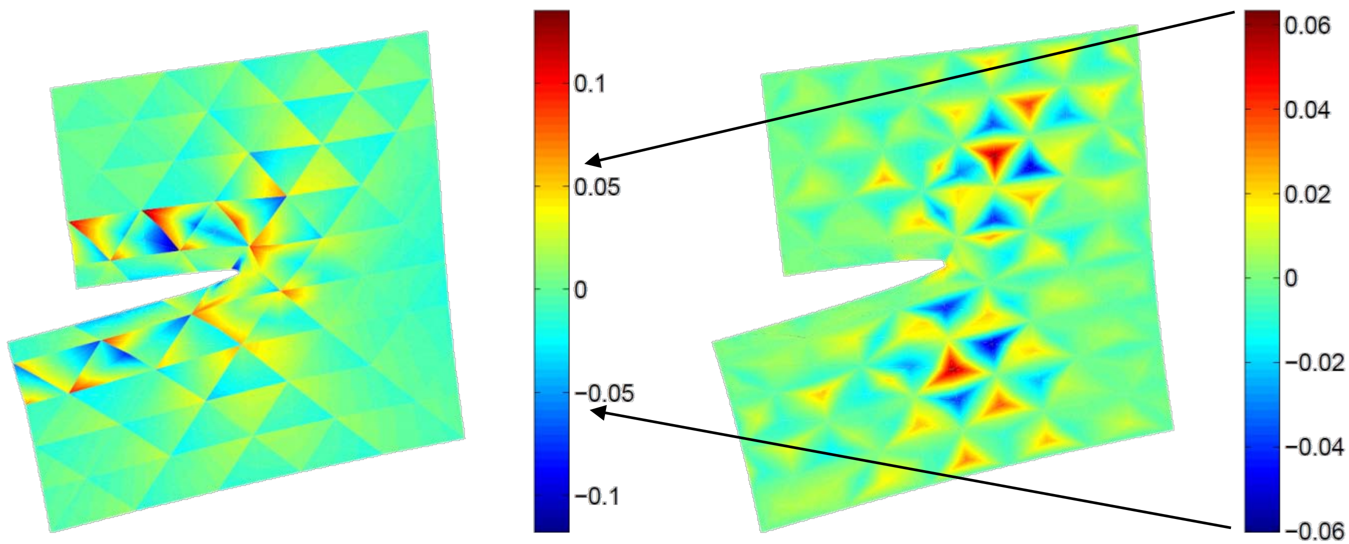

C0, 203 DOFs

C∞, 469 DOFs

Exact error dispersion: *y*-stress

topologic pattern of singular enrichment

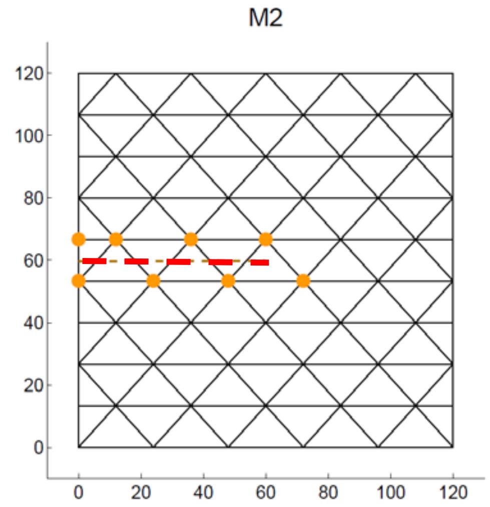

uniform polynomial enrichment,
b = 2

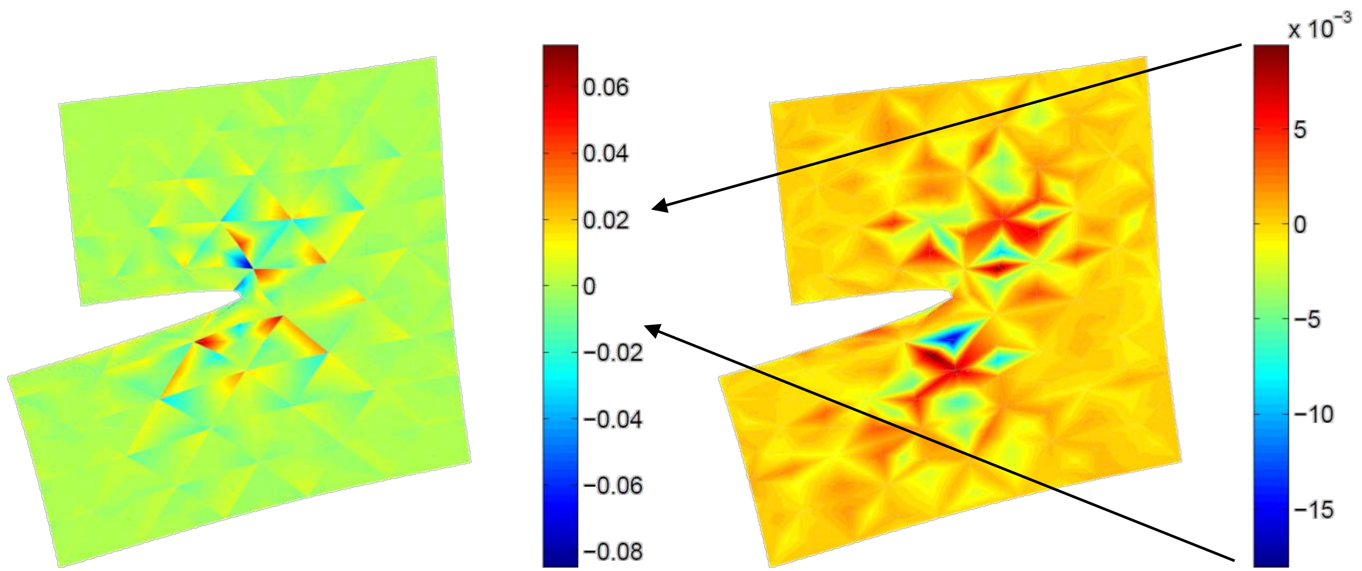

C0, 451 DOFs

C∞, 841 DOFs

WCCM XI - ECCM V - ECFD VI
BARCELONA 2014

Collecting data of the three cases…

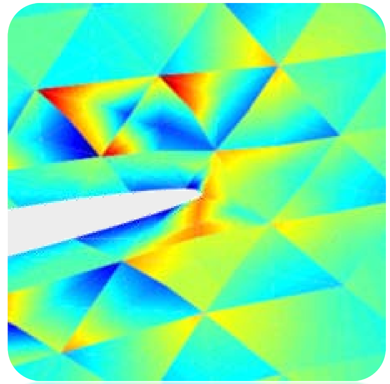

C^0

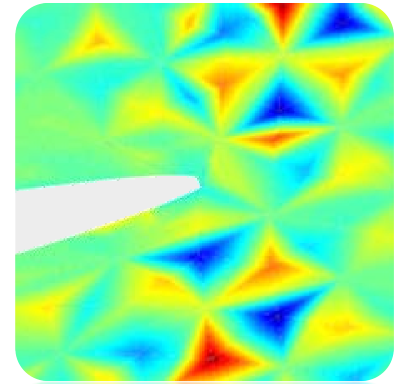

C^∞

C^0	C^∞
b=1, 191 DOFs, 145x10^{-3}	*b*=1, 451 DOFs, 62x10^{-3}
b=1, *p*=2, 203 DOFs, 130x10^{-3}	*b*=1, *p*=2, 469 DOFs, 62x10^{-3}
b=2, 451 DOFs, - 85x10^{-3}	*b*=2, 841 DOFs, - 19x10^{-3}

Angle of crack growth: θ_{ADV}

$K_I = 1.0, \; K_{II} = 1.0$

$$\sigma_x = \frac{K_I}{\sqrt{2\pi r}}\cos\left(\frac{\theta}{2}\right)\left[1-\operatorname{sen}\left(\frac{\theta}{2}\right)\operatorname{sen}\left(\frac{3\theta}{2}\right)\right] - \frac{K_{II}}{\sqrt{2\pi r}}\operatorname{sen}\left(\frac{\theta}{2}\right)\left[2+\cos\left(\frac{\theta}{2}\right)\cos\left(\frac{3\theta}{2}\right)\right]$$

$$\sigma_y = \frac{K_I}{\sqrt{2\pi r}}\cos\left(\frac{\theta}{2}\right)\left[1+\operatorname{sen}\left(\frac{\theta}{2}\right)\operatorname{sen}\left(\frac{3\theta}{2}\right)\right] + \frac{K_{II}}{\sqrt{2\pi r}}\operatorname{sen}\left(\frac{\theta}{2}\right)\cos\left(\frac{\theta}{2}\right)\cos\left(\frac{3\theta}{2}\right)$$

$$\tau_{xy} = \frac{K_I}{\sqrt{2\pi r}}\cos\left(\frac{\theta}{2}\right)\operatorname{sen}\left(\frac{\theta}{2}\right)\cos\left(\frac{3\theta}{2}\right) + \frac{K_{II}}{\sqrt{2\pi r}}\cos\left(\frac{\theta}{2}\right)\left[1-\operatorname{sen}\left(\frac{\theta}{2}\right)\operatorname{sen}\left(\frac{3\theta}{2}\right)\right]$$

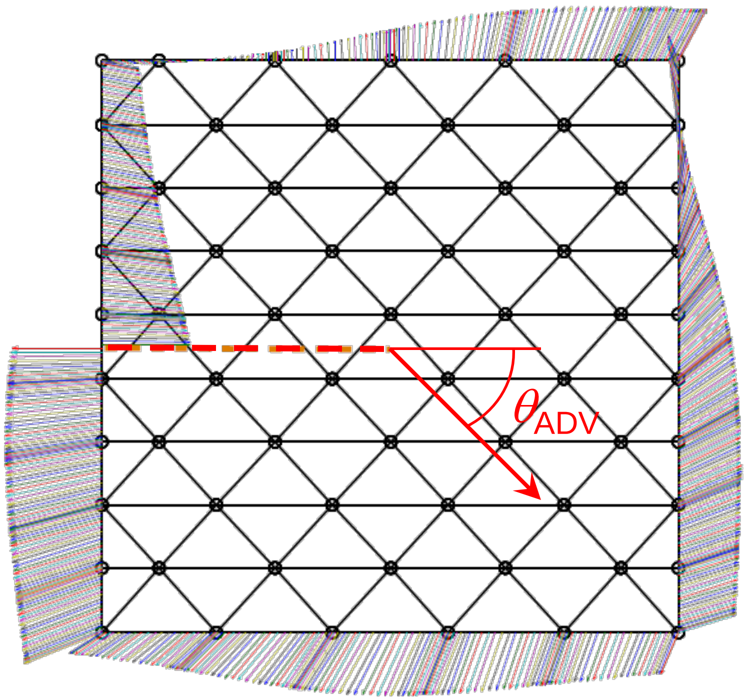

Angle of crack advance: θ_{ADV}

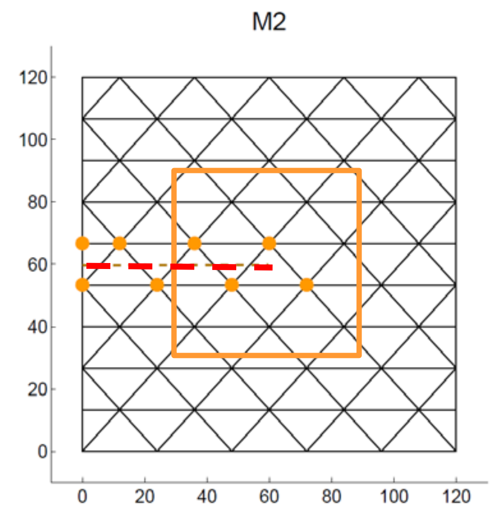

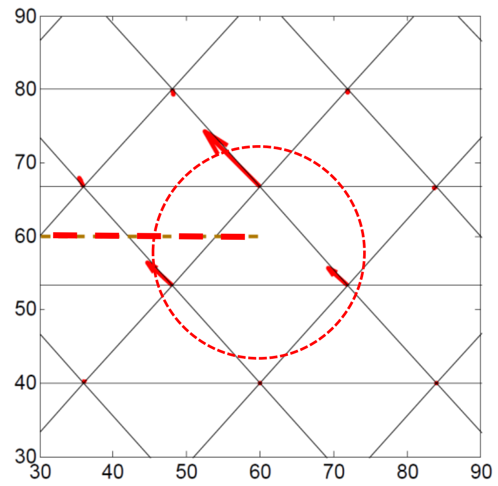

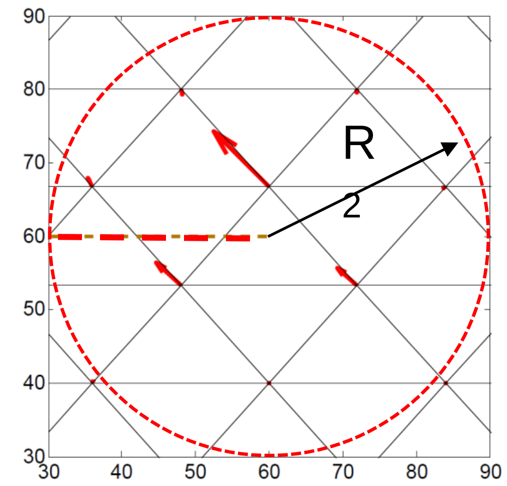

Configurational forces are restorative forces !

Angle of crack advance: θ_{ADV}, $b = 1$

Crack tip enrichment

C^0

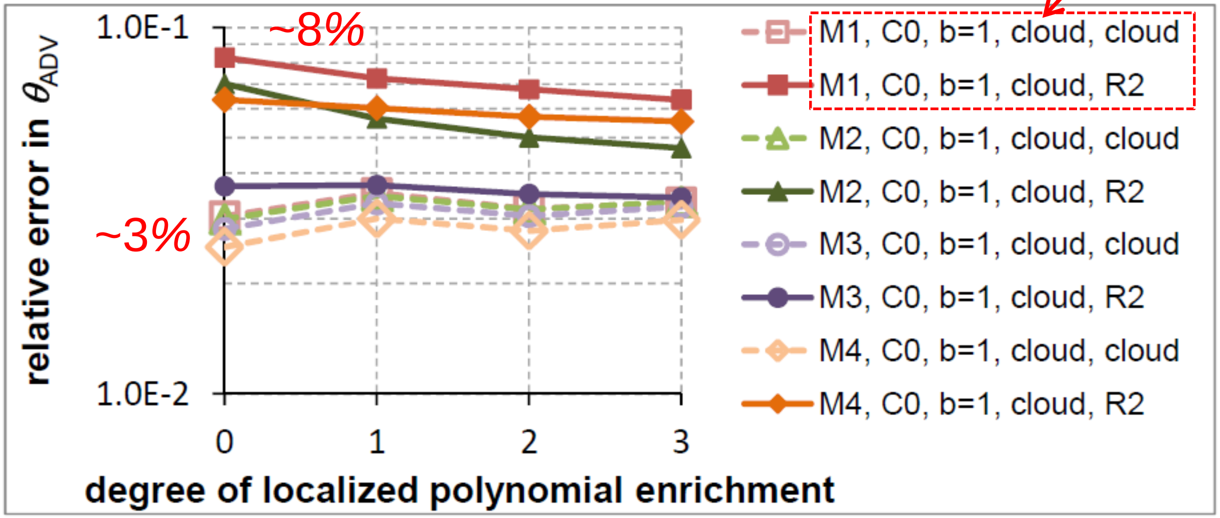

C^k

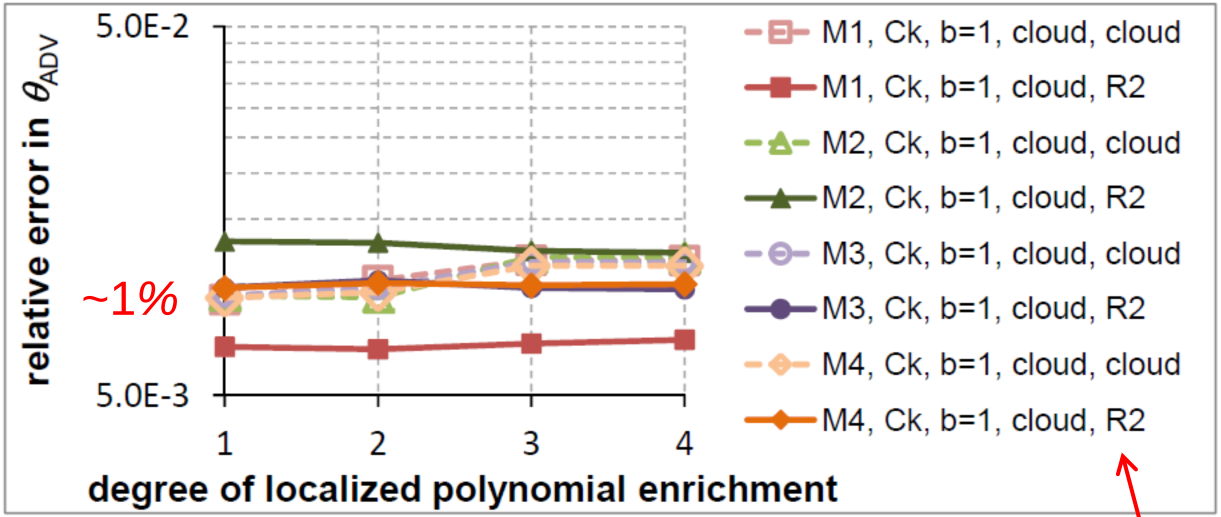

Topologic pattern of singular enrichment

Uniform polynomial enrichment, $b = 1$

Nodes for the configurational force

WCCM XI - ECCM V - ECFD VI
BARCELONA 2014

Angle of crack advance: θ_{ADV}, b = 2

C^0

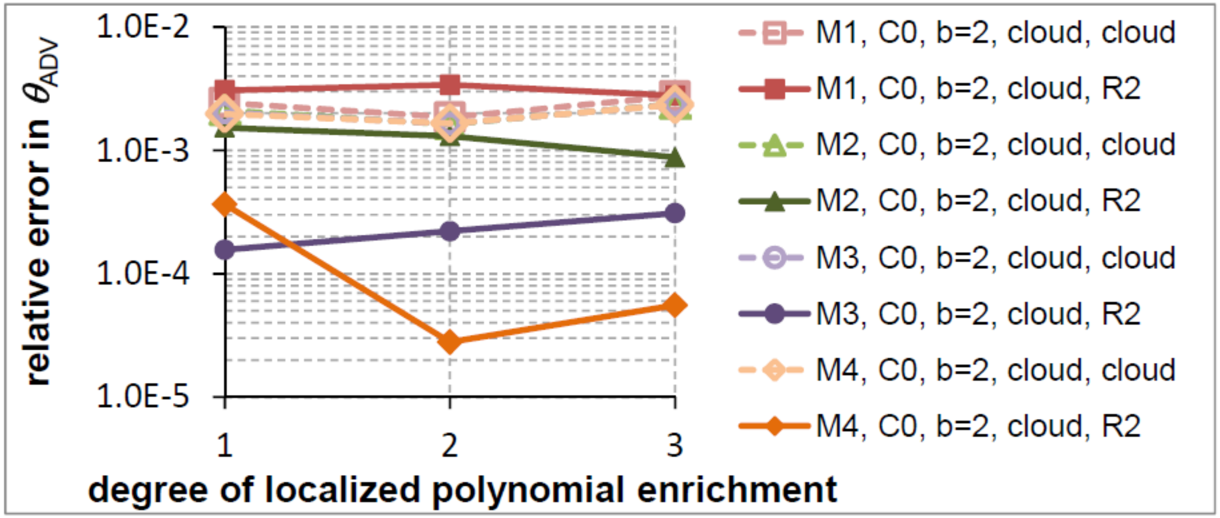

C^k

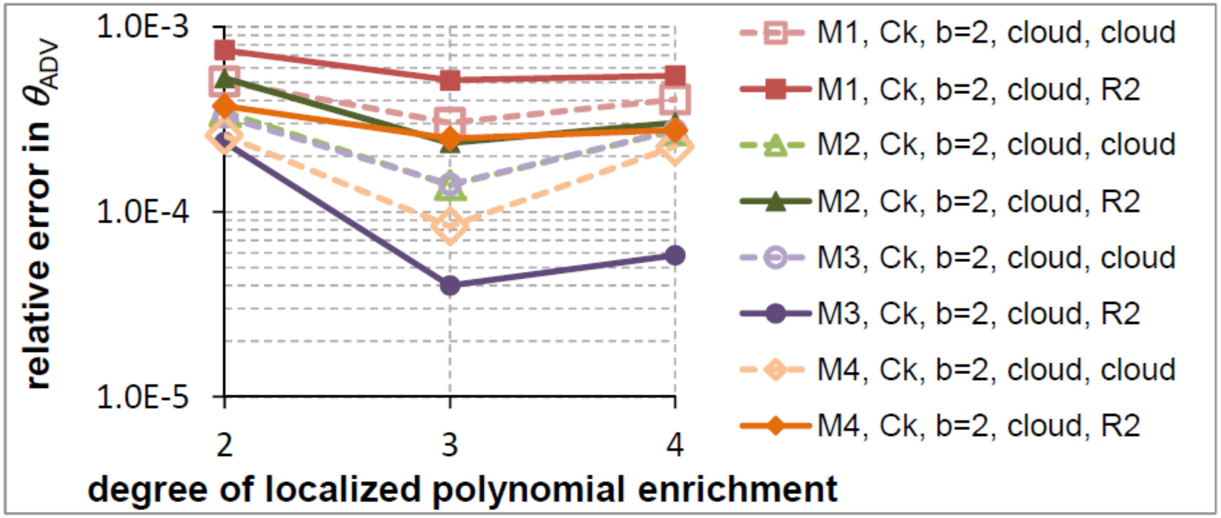

Topologic pattern of singular enrichment

Uniform polynomial enrichment, *b* = 2

Joining C^k-GFEM and C^0-GFEM

C^0 and C^k weighting functions

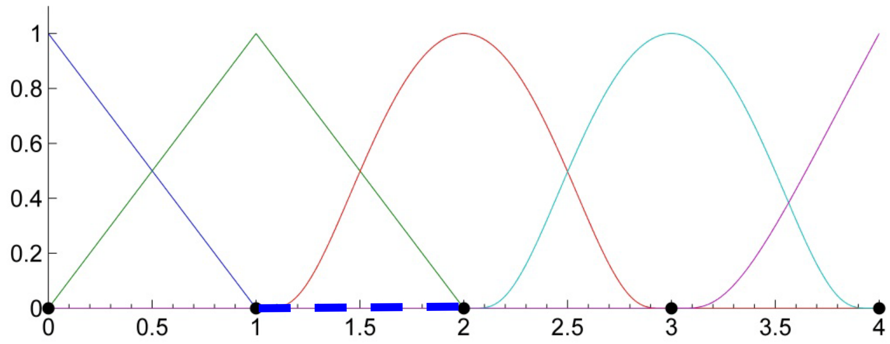

Partition of unity

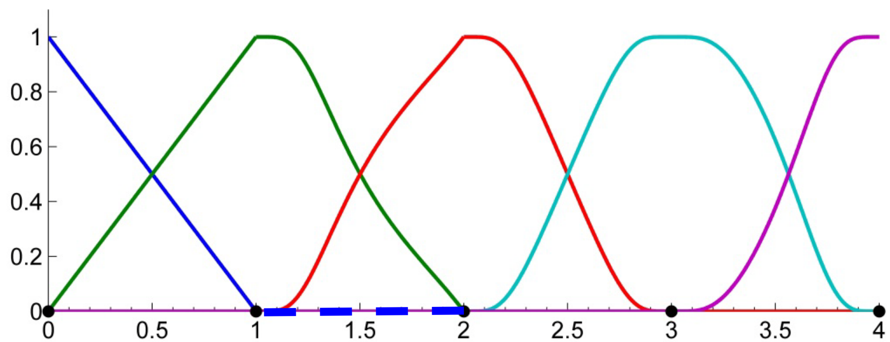

Shepard equation -> $$\varphi_\alpha(\boldsymbol{x}) = \frac{\mathcal{W}_\alpha(\boldsymbol{x})}{\sum_{\beta(\boldsymbol{x})} \mathcal{W}_\beta(\boldsymbol{x})}$$

- Straightforward!!!
- Application of smooth PoUs only where they are convenient !

Concluding remarks

C^k -GFEM shows better estimates of J and θ_{ADV} than $\boldsymbol{C^0}$ -GFEM:

- Probably due to the well determined flat-top;

- Smoothness seems to reduce transition effects around singular enrichment;

- Lower dependence with enrichment pattern;

- Lower dependence on the size of the region used to compute configurational forces;

-In general, C^k -GFEM combines:

  - Higher regularity;
  - Flat-top property;
  - Definition on global coordinates -> admits extremely distorted meshes;
  - Compact support.

Disavantages: - Lower polynomial reproducibility than C^0 -GFEM /XFEM;
- Higher integration cost;

Solution: - Apply smooth PoUs only at convenient zones of the model !

Acknowledgements

National Council for Scientific and Technological Development

Ministry of Science, Technology and Innovation of Brazil

Thank you!

mendonca@grante.ufsc.br